

Improved Ear Verification After Surgery - An Approach Based on Collaborative Representation of Locally Competitive Features

R. Raghavendra Kiran B. Raja Sushma Venkatesh Christoph Busch
Norwegian Biometrics Laboratory
Norwegian University of Science and Technology (NTNU), Gjøvik, Norway

Abstract

Ear characteristic is a promising biometric modality that has demonstrated good biometric performance. In this paper, we investigate a novel and challenging problem to verify a subject (or user) based on the ear characteristics after undergoing ear surgery. Ear surgery is performed to reconstruct the abnormal ear structures both locally and globally to beautify the overall appearance of the ear. Ear surgery performed for both for beautification and corrections alters the original ear characteristics to the greater extent that will challenge the comparison and subsequently verification performance of the ear recognition systems. This work presents a new database of images from 211 subjects with surgically altered ear along with corresponding pre and post-surgery samples. We then propose a novel scheme for ear verification based on the features extracted using a bank of filters learnt using Topographic Locally Competitive Algorithm (T-LCA) and comparison is carried out using Robust Probabilistic Collaborative Representation Classifier (R-ProCRC). Extensive experiments are carried out on both clean (normal) and surgically altered ear database to evaluate the performance of the proposed ear verification scheme. We also present a comprehensive performance analysis by comparing the performance of the proposed ear recognition scheme with eight different state-of-the-art ear verification system. Furthermore, we also present a new scheme to detect both deformed and surgically altered ear using one-class classification. Experimental results indicate the magnitude of problem in verifying the surgically altered ears and the signifies the need for considerable research in this direction.

Keywords: Ear recognition, Surgery, Locally Competitive Algorithm, Collaborative Representation

1. Introduction

With the widespread use of access control systems that insist the user authentication, biometrics based systems are increasingly becoming popular. Biometric systems employ physical and/or behavioural characteristics of the individual to automatically identify/verify the access control. Among the different biometric characteristics, the 2D ear (or outer ear) has long been recognized as the potential biometric characteristics for the identification/verification of a person. The 2D ear biometrics exhibit an appealing feature to have unique shape and structure (even among twins) [1] that can be captured without subject cooperation, not often affected by the facial expression and demonstrated significant identification accuracy, especially in the controlled conditions. These features have contributed to the 2D ear recognition to elevate them as the promising biometric characteristics for both biometric and forensic applications.

The 2D ear recognition was first investigated by French criminologist Alphonse Bertillon in 1890 [2]. One of the interesting earlier works was carried out by the American police officer Alfred Iannarelli [1] on more than 10,000 ear images using 12 different features to identify the data subjects successfully. Alfred Iannarelli also conducted a study on the ear from twins and triplets that demonstrated the unique properties of the ear among twins and triplets [1]. With the growing progression of biometrics, the machine vision researchers have started addressing the ear recognition from past decade. This has resulted in a significant amount of research work in both (1) ear detection (2) ear feature extraction and comparison technique that improved the overall performance of the ear recognition system.

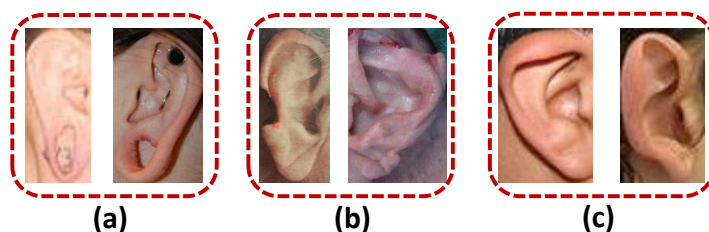


Figure 1: (a) Ear with deformed ear lobe; (b) Ear with Structural impairment; (c) Ear with disfiguring defects

Ear detection is the primary step in the ear recognition system that has received prominent attention from the researchers. Several approaches have been proposed

that include both manually assisted and completely automatic methods to achieve ear detection and segmentation. The manually assisted ear segmentation is introduced in [3] that allows to mark manually the landmarks on the ear displayed on the computer. These landmarks are further used by the computer software to segment the ear. The template based approaches using deformable contours [4], edge detectors [5], morphological operations [6] and hybrid approaches [7] based on pyramids and sequential similarity computation is also explored. Template based approaches have shown significant improvement in the ear segmentation accuracy but show the degraded performance especially in the unconstrained conditions. Shape-based 2D ear segmentation involves in finding the elliptical shape of the ear using Hough transform and it was introduced in [8]. As the shape-based segmentation schemes are based on the edge information, these methods are prone to noises that are encountered in the unconstrained scenario. Hybrid approaches that combine more than one method are: skin color detection combined with template based approaches [9], Gabor jets combined with Principal Component Analysis (PCA) [10], ray transforms combined with a shape based approaches [11] and color information combined with edge extracted from range images [12]. Lastly, the classifier-based approach using Haar features and Adaboost techniques was proposed in [13]. This method is further improved by [14] to detect ear with varying pose, noise, and in presence of multiple ears.

Ear feature extraction and comparisons are widely addressed to develop both robust and accurate ear recognition system. Various feature extraction methods are proposed that can be broadly classified into three sub-classes, namely: global approaches, local approaches and hybrid approaches. The global approaches include sub-space approaches such as Principal Component Analysis (PCA), Linear Discriminant Analysis (LDA), Independent Component Analysis (ICA), Sparse Representation Classifier (SRC) [15], Fuzzy rules [16] and Kernel Discriminant Analysis (KDA). Texture based approaches include Gabor filters, Local Binary Patterns (LBP), Local Phase Quantisation (LPQ), Binarised Statistical Image Features (BSIF), wavelet transform, log-Gabor filters, Shape-based Force field transformations and Voronoi distance graph. The local features include the use of SIFT, SURF and landmark points. The Hybrid approaches combine more than one feature extraction techniques. Recently, the use of Convolutional Neural Network (CNN) was explored for the ear recognition that has demonstrated the improved results when compared with both shape and texture based techniques. However, the effectiveness of the CNN depends on the availability of the large scale ear database. The ear recognition for the new born infants are addressed in [16], [17]. The popularity of 2D ear biometrics also resulted in many survey papers such

as [18], [19] [20], [21], [22], [23], [24] and they provide the complete overview on the tools and techniques developed for accurate 2D ear recognition.

1.1. Surgical alteration of ears

The popularity of ear characteristics in biometrics is now challenged by the problem of surgical alteration for many reasons such as enhancing the beauty and correcting deformed ears by birth or as a result of accident. The increasing interest in beautification through a surgery is seen mainly in the developed countries. The goal of these surgeries is to improve the appearance (or correcting the defects) of the human body parts to enhance the beauty of the body parts. The beautification surgery is most commonly performed on face, ear, nose and lips that are driven by the availability of the affordable cost technology. The ear surgery is gaining popularity and the recent statistics released by American Society of Aesthetic Plastic surgery for year 2009 ¹ report around 29000 ear surgeries in US alone. Among these 61% are woman and 39% are men undergoing ear surgery. The possible reasons for the ear surgery include:

1. The prolonged use of large and heavy earrings that can stretch and tear the ear lobe.
2. Structural impairment caused due to accidents.
3. Correcting disfigured defects by birth.

Figure 1 shows the example of deformed ears as a result of wearing heavy ear-rings that has resulted in deformed ear lobe (see Figure 1 (a)), structural impairment (see Figure1 (b)) and disfiguring defects (see Figure 1 (c)). Even though the 2D ear recognition is well addressed problem, the presence of both deformed and surgery ear will introduce new challenges especially on the accuracy of the ear recognition.

The primary objective of this paper is to assess and address the challenges of surgically altered ear in achieving accurate verification performance and also present the comprehensive evaluation of the nine different state-of-the-art ear recognition algorithms. Since ear surgery will change both local as well as the global appearance of the ear characteristic to greater extent, it's hard to find the correlation between pre- and post-operated ear. With this backdrop, in our previous work [25], we made the preliminary study on evaluating the ear recognition algorithms, especially on the ear lobe surgery database comprised of 44 subjects.

¹<http://www.realself.com/asps-ear-surgery-statistics>

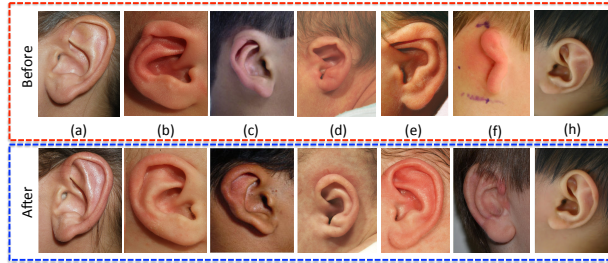


Figure 2: Illustration of different kind of ear surgeries; The images inside the red dashed line correspond to the images taken prior to surgery while the images inside blue dashed line depict the images taken after the surgical procedure. The images for each correction is placed below each of the corresponding image before surgery. (a) Antihelical fold correction; (b) Constricted ear correction; (c) Cryptotia correction in upper lobe; (d) Cup ear correction; (e) Lop ear correction; (f) Microtia correction; (g) Stahl ear correction

Further, we have also introduced the new approach for 2D ear recognition based on the hybrid fusion of block-wise texture features extracted using Local Phase Quantization (LPQ) and Histogram of Oriented Gradients (HoG) to mitigate the effect of ear lobe surgery and to marginally improve the reliability of 2D ear recognition systems.

In this paper, the same work is extended in many directions. By introducing a new large-scale 2D ear surgery database comprised of 211 subjects with three different kinds of surgeries: (1) Earlobe surgery, (2) Helical surgery and (3) Otoplasty. We then present a novel algorithm for reliable verification of surgically altered ears using a set of naturally learned feature descriptors through Topographic Locally Competitive Algorithm (T-LCA) [26] [27] [28] in an unsupervised manner. These learned filters are then used to extract the invariant features from the surgically altered ears that are further classified using Robust Probabilistic Collaborative Representation Classifier (R-ProCRC) [29]. The proposed feature extraction and classification scheme has demonstrated an outstanding performance on both surgically altered ear database and non-surgical (normal) 2D ear database that shows the significant improvement in performance on both cases. Lastly, we propose a new scheme based on 1-class SVM classifier to identify the deformed ear (before surgery). Overall, the main contributions of this work can be listed as below:

- A comprehensive work that adds a new dimension to 2D ear recognition by discussing the challenges of ear surgery and systematically evaluating the biometric performance of existing 2D ear recognition algorithms on a

surgically altered 2D ear database.

- New large-scale database of surgically altered ears obtained from 211 subjects with three different kinds of procedures: earlobe, helical (both mid and top) and otoplasty. This new database is acquired to have 2D ear images before and after surgery for corresponding subjects. Each ear in the database have one image prior-surgery and one image post-surgery. The magnitude of problem increases not only due to surgical changes but also due to single reference samples i.e, single-sample classification problem.s
- A novel scheme for 2D ear verification using naturally inspired features learned using T-LCA and R-ProCRC that can adequately capture the invariant features to improve the overall verification performance on both surgically altered ear database and non-surgical (or traditional) 2D ear database. More precisely, we show that proposed scheme is robust on all three different kinds of ear surgery even when there is only one sample enrolled for ear.
- Proposed a new scheme to detect both deformed and surgically modified ears using Local Phase Quantization (LPQ) and 1-class Support Vector Machine (SVM).
- Extensive experiments are carried out to evaluate the performance of the proposed scheme along with nine different state-of-the-art ear verification techniques including the *Deep – Learning* method based on pre-trained deep-network (*AlexNet*).
- Achieving improved performance using the proposed 2D ear recognition scheme on both, surgically altered and non-surgical ear database when compared with nine different state-of-the-art schemes.

The rest of the paper is organised as follows: Section 2 presents the detailed description on ear surgery in particular to correct earlobe, helix and beautification. Section 3 provides the details on database and experimental protocols. Section 4 presents the proposed scheme for improved 2D ear recognition after ear lobe surgery and Section 5 presents the proposed deformed ear detection scheme. Finally, Section 6 presents the quantitative results and Section 7 draws the conclusion.

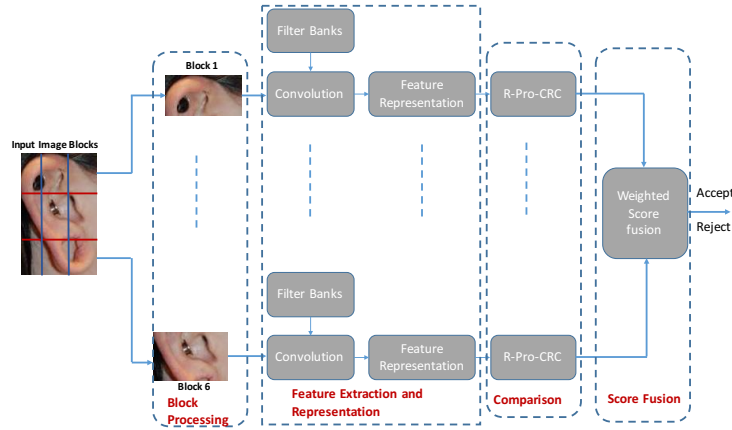


Figure 3: Block diagram of the proposed ear surgery verification scheme

2. Ear Surgery

This section gives a brief overview of external anatomy of the ear and different kind of procedures performed on the ear to correct various deformities and/or to beautify it. The external structure of ear is constituted by helix, antihelix, legs of helix, legs of antihelix, tragus, antitragus and the lobe along with the depressions called scapha, triangular fossa, concha and intertragical notch. Various surgical procedures are carried out on local structures of ear to correct the deviation from the standard structure of the ear and also to enhance the beauty of the ear which is commonly known as Otoplasty. Further, Earlobes are surgically repaired to fix the torn, enlarged, punctured earlobes resulting from the long usage of heavy jewellery or trauma [30]. The surgical procedure results in a permanent change of shape and appearance of the earlobe along with the global structure and texture of the ear. Another important class of surgery on external ear is the procedure performed on helical part of the ear. The most common cause for the helical surgery is the congenital ear deformities which often require surgical correction for both aesthetic and psychological reasons. Another class of surgeries are performed to correct prominent ears resulting due to auricular malformation along with many other deformities, such as constricted ears, macrotia, helical rim deformities. Figure 2 depicts the various categories of the helical corrections done to the ear.

Note: The detailed explanation of different type of surgical procedures are provided in the supplementary document for the interested readers.

3. Ear Surgery Database

The major challenge posed in this work was to prepare a surgically altered ear database, such that for each enrolled ear instance there exists a sample before and after the ear surgery. To the best of our knowledge, there is yet no publicly available ear surgery database that will allow the biometric researchers to understand the impact of ear recognition algorithms and also to develop new techniques to overcome this challenge. Thus, it is crucial to collect the 2D ear surgery database such that, each data subject will have 2D ear image captured before and after surgery.

Inspired from the earlier data collection procedure followed in face plastic surgery database [31], Labelled Face in Wild (LFW) [32] and many others, we downloaded the real-world pre-surgery and post-surgery ear images corresponding to the same individual from several web-pages. All the surgery images are manually selected to assure the presence of full ear in pre-surgery and post-surgery scenario. Our database is comprised of 211 subjects with both pre-surgery and post-surgery ear images. For each data subject, there are two frontal ear images with proper illumination are collected such that the first is taken before surgery and the second is taken after surgery. Thus, the whole database consists of $211 \times 2 = 422$ 2D ear samples. The database contains three main varieties of cases such as: ear lobe surgery (52 subjects), helical surgery (39 Subjects), ear beautification surgery (120 subjects).

Figure 1 and Figure 2 show the examples of different variety of the deformed ear samples before and after surgery. It can be visually observed that the surgical procedure will alter the overall appearance of the ear image both locally and globally that can degrade the performance of the existing ear verification algorithms. In addition to surgical alterations, the database also poses challenges in terms of image quality because of the heterogeneous nature of capture devices (different make and manufacture, varying image resolutions) and the limited number of samples per subject (only two samples per ear where one sample is collected before surgery and another after surgery). These facts are observed with all three variety of the ear surgery cases considered in this work. Our database is made available to the research purpose, and interested researchers are asked to contact the authors for availing the database.

4. Proposed Ear recognition scheme

Figure 3 shows the block diagram of the proposed scheme for robust ear recognition. The primary objective of the proposed scheme is to explore the naturally

learned feature descriptors using the T-LCA [26] [27] [28] in an unsupervised manner. The learned feature descriptors are known to capture the invariant features from the images that in turn can be used to extract the discriminant features for robust ear verification. The proposed scheme can be structured in the following functional units:

4.1. Block processing

Given the ear image I , we divide the whole image into six non-overlapping blocks $I_{B1}, I_{B2}, \dots, I_{B6}$. In this work, we intend to follow the block based approach to effectively address the distortion before and after surgery of the ear. The surgical procedure majorly alters operated area (except in the case of the completely deformed ear) while retaining the global appearance of the ear. Hence, the use of the block based approach can preserve the unique information that is not altered during the surgical process. In this work, we consider only six blocks such that, we divide the whole image into three non-overlapping horizontal blocks and three non-overlapping vertical blocks. Each of these blocks is processed independently using feature extraction, representation and comparison modules as explained below.

4.2. Feature Extraction and Representation

In this work, we explore the feature (or dictionary) learning approach to learn the feature descriptors that are used to extract the features from the given i^{th} block I_{Bi} of ear image image I . The problem of feature learning is a well explored area in which several approaches based on the unsupervised learning using sparse decomposition is proposed [33] [28] [26] [34] [35]. The primary objective of these unsupervised learning is to find a unique dictionary (or filter-banks or code-books) that will form a basis function to extract the features from the given image. Among the various approaches, the Local Competitive Algorithms (LCA) appear to be appealing since it is based on exploring the neurally plausible sparse coding mechanism that can learn the invariant features (or filter banks or dictionary). The LCA also utilizes the node (dictionary elements are referred as nodes) dynamics based on the principles of thresholding and local competitions that are less computational when compared to greedy algorithms [26].

The LCA belongs to the class of neurologically inspired algorithms that can be described using a set of non-linear Ordinary Differential Equations (ODE). Given the input signal s and the pseudo-overcomplete dictionary ϕ , the LCA model approximates the input s as a linear combination of sparse vector and the dictionary elements as follows [28] [34]:

$$\hat{s} = \sum_m a_m \phi_m \quad (1)$$

Where, ϕ is the N-by-M matrix where columns are the dictionary elements $\phi_m \in \mathbb{R}^N$, $m = 1, \dots, M$; $\phi = [\phi_1, \dots, \phi_M]$. The dictionary elements are commonly referred as nodes or neurons or atoms.

The sparse co-efficient vector a is determined by solving the LCA algorithm that can be written in the matrix formulation as follows [28]:

$$u(\hat{t}) = \frac{1}{\tau} [b - u(t) - (\phi^t \phi - I)a(t)] \quad (2)$$

Where, $b = [b_1, \dots, b_M]^t = \phi^t s$ are the driving inputs and reflect how well the signal matches different nodes. The closer the signal to a node, the bigger is the corresponding driving value. $u(t) = [u_1(t), \dots, u_M(t)]^t$ are the function representation of time-varying internal states of the system at time t . In LCA, a non-linearity is introduced in the form of a threshold function T_λ to guarantee that small internal states that do not add much information and is approximated to zero. $a(t) = [a_1(t), \dots, a_M(t)]^t = T_\lambda(u(t))$ represents the sparse co-efficients vector.

In this work, we explore the dictionary learning using two layer LCA that is termed as T-LCA. The T-LCA will first initialize in the layer-1 and then projected to the layer-2 in a feed forward manner where LCA is performed. Then, the activity coefficients computed in the layer-2 is projected back to the layer-1, and then LCA is again performed. The use of topographical structure will mitigate the perturbation of the input signal and thus the optimal dictionary (of filters) with invariant properties can be learned using T-LCA. To effectively learn the dictionary (or filter banks), we begin with the dataset comprised of small patches of size 16×16 that are randomly sampled from 10 different natural images[36]. We have used 100,000 images patches that are preprocessed by subtracting the mean of each image patch itself to remove the DC component. Since we are using the image patch size $16 \times 16 = 256$ and the number of atoms (or neurons) as 256, the dictionary (ϕ) will result in dimension of 256 filters of size 16×16 . We begin with random initialization of the dictionary atoms which are then optimized following the image patched in an iterative way using T-LCA Algorithm.

Figure 4 shows the features (or filters or dictionary elements) learned by T-LCA that shows the similar characteristics to those of Gabor-like edge detectors. Further, it is also interesting to note that the distribution of these filters is very

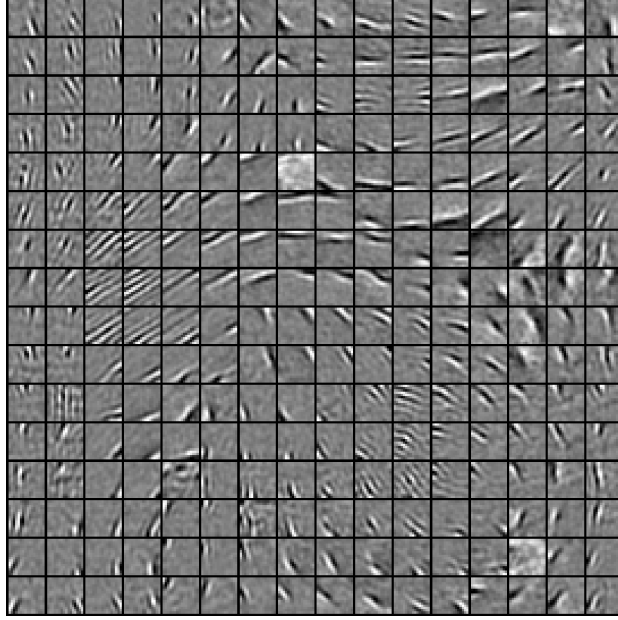


Figure 4: T-LCA filter bank (or dictionary or receptive fields).

localized. Thus, the use of T-LCA can learn the significant features and simpler to implement, fast to run and does not require time-consuming tuning of hyperparameters. Thus, it is our intuition that the use of these filter banks learned using T-LCA as the feature extraction techniques for the surgery ear will allow one to capture the invariant features that will allow improving the verification performance.

In the next step, we perform the feature extraction by convolving the i^{th} block of ear image I_{Bi} with each of the 256 filters that are learned using T-LCA. The feature extraction can be represented as follows:

$$F_{ki} = I_{Bi} * FB_k; \quad \forall k = 1, 2, \dots, 256, \quad \forall i = 1, 2, \dots, 6 \quad (3)$$

Where, $*$ represents the convolution operation and F_{ki} represent the convolution result with k^{th} filter with i^{th} ear image block I_{Bi} . Figure 5 (c) illustrates the qualitative results corresponding to the response of the T-LCA filter bank to the ear image block I_{Bi} .

Since the feature extraction technique is computationally tedious with 256 responses, we propose a two step process that can efficiently represent these extracted features. The adopted approach will first binarize the each convolved im-

age (F_k) by comparing each pixel to the present threshold as follows:

$$B_{ki}(x, y) = \begin{cases} 1, & \text{if } F_{ki}(x, y) \geq 0 \\ 0, & \text{Otherwise} \end{cases} \quad (4)$$

Where, (x,y) represents the pixels location and $B_{ki}(x, y)$ represents the binarized convolved image with k^{th} filter and i^{th} ear image block .

In the next step, we represent the binarized images to form a code image by stacking 8 images each to construct a binary code of 8 bits as follows:

$$C_{il} = \sum_{k=1}^8 B_{ki} \times 2^{k-1}; \quad \forall l = 1, 2, \dots, 32 \quad (5)$$

Where C_{il} represent the 8-bit binary code for l^{th} stack of 8 images. Since there are 256 convolved image, we will have 32 (= 256/8) different 8 bit representation. C_{il} is also known as code image. Figure 5 (d) shows the qualitative illustration of the code images C_{il} .

Following the previous step, we further process the coded image C_{il} to obtain the time and frequency representation using Short-Term-Fourier-Transform (STFT) to better represent the localized edge features obtained using t-LCA filter bank. The local time and frequency responses are computed in a local window W as given by Equation 6:

$$FT_{il}(u, v) = C_{il}(x, y)W_R \exp\{-j2\pi U^T y\} \quad (6)$$

where W represents the window and U represents the frequency at which local Fourier response is computed. In this work, the local Fourier coefficients are computed for the frequency points $u_1 = [a, 0]^T$, $u_2 = [0, a]^T$, $u_3 = [a, a]^T$ and $u_4 = [a, -a]^T$ [37].

The obtained frequency information present in the form of Fourier coefficients is further separated into real and imaginary parts for each component in Fourier response $[Re\{FT_{il}\}, Im\{FT_{il}\}]$ to form a final vector R_{il} which is further as given by Equation 7.

$$b_{il} = \begin{cases} 1, & \text{if } R_{il} > 0 \\ 0, & \text{otherwise} \end{cases} \quad (7)$$

The quantized coefficients are represented as integer value Q_{il} in the range of 0 – 255 by using simple binary to decimal conversion strategy as given by

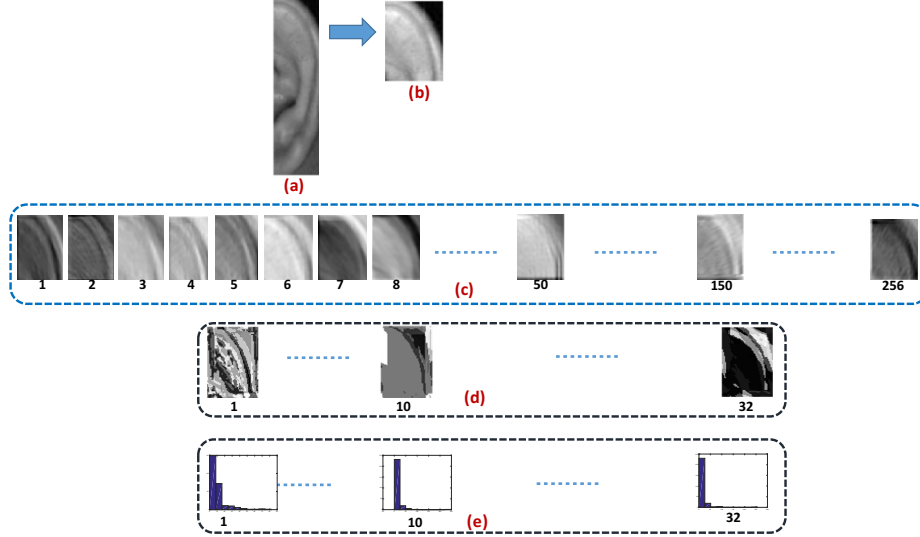


Figure 5: Qualitative results of the Proposed feature extraction scheme (a) Input ear image (b) Ear Block (c) T-LCA repose images (d) Coded image (e) time-frequency histograms

Equation. 8.

$$Z_{il} = \sum_{j=1}^8 b_{ilj} \times (2^{(j-1)}); \quad (8)$$

Where $j = 1 \dots 8$ corresponds to 4 real and 4 imaginary frequency coefficients.

We represent Z_{il} by using the histogram representation as given below:

$$H_{il} = \sum_{e=0}^{256} (Z_{il})_e; \quad \forall l = 1, 2, \dots, 32 \quad (9)$$

Where, H_{il} represents the histogram with a dimension of 1×256 corresponding to l^{th} stack image. Figure 5(e) illustrates the histograms obtained using Equation 9.

Finally, the histogram features from all 32 stacked binary codes H_{il} are concatenated to form the single feature vector F_i as follows:

$$X_i = [H_{i1} || H_{i2} || \dots || H_{i32}] \quad (10)$$

Thus, for the each block of the ear image I_{Bi} , the proposed feature extraction

Algorithm 1 Proposed ear feature extraction and comparison scheme

```
1: Input: Ear Image  $I$ ; Filter bank learned from T-LCA
2: Variables:  $k$  // Number of subjects and  $i$  is the number of image blocks.
3: Initialization:  $X_i = \text{zeros}(N_f, k)$ .
4:  $k = 211$  // Number of subjects.
5:  $N_f = 8192$  // Length of features.
6:  $i = 6$  // Number of image blocks.
7: Step 1: Obtain six ( $i$ ) independent image blocks from ear image  $I$ .
8: for  $i = 1$  : Number of image blocks do
9:   for  $j = 1$  : Number of subjects do
10:     Step 2: Compute the features  $F_i$  according to Equation 10.
11:     Step 3: Append  $F_i$  as the column of  $X_i$ 
12:   end for // Number of subjects
13:   Output: Feature matrix  $X_i$  corresponding to  $i^{\text{th}}$  ear block.
14:   Step 4: Given the probe image block  $y_i$ .
15:   Step 5: Get the comparison score using R-ProCRC according to Equation
16:     19.
17:   Step 6: Repeat Step 1 - Step 5 for all blocks  $i$ .
18: end for // Number of image blocks
Output: Comparison scores  $C_i, \forall i = 1, 2, \dots, 6$ .
```

and representation will result in feature dimension of 8192 ($= 32 \times 256$).

4.3. Comparison

In this work, we employ the Robust Probabilistic Collaborative Representation Classifier (R-ProCRC) [29] to obtain the comparison score. Given the reference samples with i^{th} ear image block from k number of subjects can be represented as: $X_i = [X_{i1}, \dots, X_{ik}]$ and the corresponding labels l_x . Then, each data point x can be represented as the linear combination of collaborative subspace s as: $x = X_i \alpha$, where α is the representation vector. The intuition behind R-ProCRC[29] is to formulate s as the probabilistic collaborative space such that, different data points x have different probabilities of $l(x) \in l_x$ that can be defined using Gaussian function as follows [29]:

$$P(l(x) \in l_x) \propto \exp(-c \|\alpha\|_2^2) \quad (11)$$

Given the test sample y_i corresponding to the same ear block i of the reference samples, the probability that y_i belongs to l_{X_i} , i.e., $P(l(y_i) \in l_{X_i})$ can

be measured by finding a data point x in s and then compute two probabilities: $P(l(x) \in l_x)$ and the probability that y_i has the same class label as x , i.e. $P(l(x) = l(y_i))$ that are formulated as follows [29]:

$$P(l(y_i) \in l_{X_i}) = P[l(y_i) = l(x)|l(x) \in l_{X_i}].P(l(x) \in l_{X_i}) \quad (12)$$

$P[l(y_i) = l(x)|l(x) \in l_{X_i}]$ can be measured by the computing the similarity between x and y_i using the Laplacian kernel as follows [29]:

$$P(l(y_i) = l(x)|l(x) \in l_{X_i}) \propto \exp(-\kappa\|y_i - x\|_1) \quad (13)$$

From Equation 11, Equation 12 and Equation 13, it follows that [29]:

$$P(l(y_i) \in l_{X_i}) \propto \exp(-\kappa\|y_i - X_i\alpha\|_1 + c\|\alpha\|_2^2) \quad (14)$$

Where, κ is a constant.

The maximum probability $P(l(y_i) \in l(X_i))$ can be obtained from the above Equation 14 as [29]:

$$\max P(l(y_i) \in l(X_i)) = \max \ln(P(l(y_i) \in l(X_i))) \quad (15)$$

The above equation provides a probability representation of y_i over the collaboration subspace s . However, to perform the classification of the probe samples y_i corresponding to subject k , the R-ProCRC will estimate the probability of y_i to each class-specific sub-space that can be represented as [29]:

$$\hat{\alpha} = \arg \min_{\alpha} \left\{ \|y_i - X_i\alpha\|_1 + \lambda\|\alpha\|_2^2 + \frac{\gamma}{K} \sum_{k=1}^K \|X_i\alpha - X_{ik}\alpha_k\|_2^2 \right\} \quad (16)$$

where, K indicates the joint probability $P(l(y_i) = 1, \dots, l(y_i))$. The first two terms in the above Equation 16; $\|y_i - X_i\alpha\|_1 + \lambda\|\alpha\|_2^2$ indicates the collaborative representation form that find a data point $x = X_i\alpha$ that is close to y_i in the collaborative subspace s . The third term $\sum_{k=1}^K \|X_i\alpha - X_{ik}\alpha_k\|_2^2$ find inside each subspace of class k a point $X_{ik}\alpha_k$ which is close to the common point x . The parameters γ and λ will act as the weights for these tree terms, which can be set based on the prior knowledge or though the cross validation.

The solution to the Equation 16 is obtained using the Iterative Reweighted

Algorithm 2 Weight optimisation using greedy algorithm

Input:

2: Comparison scores C_i , $\forall i = 1, 2, \dots, 6$ // Comparison scores obtained individually for each ear image block I_{Bi}

Variables:

4: N ; // Number of iteration. $w_i \forall i = 1, 2, \dots, 6$ // weights $GMR_{FMR@10^{-1}}$
// Genuine Match Rate (GMR) at False Match Rate (FMR) of 10^{-1} $Best - GMR_{FMR@10^{-1}}$ // Best GMR value obtained during iteration W_{Opt} // Optimized weights corresponding to best GMR

Initialization:

6: $N = 1000$ $w_i = rand(1, 6)$ such that $\sum_{i=1}^6 w_i = 1$ // Random initialization of weights $Best - GMR_{FMR@10^{-1}} = 0$; // Initialize to zero $Iter_{count} = 0$
// Initialize intermediate counter of iteration $W_{Opt} = zeros(1, 6)$ // initialize best weights to zero

while ($Iter_{count} \leq N$) and ($GMR_{FMR@10^{-1}} < Best - GMR_{FMR@10^{-1}}$)
do

8: With initialized weights w_i compute the weighted SUM rule according to the Equation 20.

 Compute the False Match Rate(FMR) and False Non-Match Rate (FNMR).

10: Compute the Genuine Match Rate(GMR) as $1 - FNMR$ at $FMR = 10^{-1}$.
 let this be: $GMR_{FMR@10^{-1}}$

12: **if** ($GMR_{FMR@10^{-1}} > (Best - GMR_{FMR@10^{-1}})$) **then**

$Best - GMR_{FMR@10^{-1}} = GMR_{FMR@10^{-1}}$ // update GMR value

14: $W_{Opt} = w_i$ // update weights value

end if

16: **end while**

Output: Optimized weights W_{Opt}

Least Square (IRLS) technique. The probability $P(l(y_i) = k)$ can be computed by:

$$P(l(y_i) = k) \propto \exp(-(\|y - X_i \hat{\alpha}\|_1 + \lambda \|\hat{\alpha}\|_2^2 + \frac{\gamma}{K} \|X_i \hat{\alpha} - X_{ik} \hat{\alpha}_k\|_2^2)) \quad (17)$$

Since $(\|y - X_i \hat{\alpha}\|_1 + \lambda \|\hat{\alpha}\|_2^2)$ is same for all subjects, it is discarded in computing $P(l(y_i) = k)$. Let

$$p_k = \exp(-(\|X_i \hat{\alpha} - X_{ik} \hat{\alpha}_k\|_2^2)) \quad (18)$$

Then, the classification is formulated as follows:

$$l(y_i) = \underset{x}{\operatorname{argmax}} p_k \quad (19)$$

The outcome of the Equation 19 is used as the comparison score to evaluate the performance of the proposed scheme for robust ear verification. We carry out the above mentioned steps for all six blocks as illustrated in the Figure 3 to obtain the comparison scores $C_i, \forall i = 1, 2, \dots, 6$ corresponding to each block. Finally, the comparison scores C_i is fused using weighted sum rule as explained in the following section.

4.4. Score fusion

In this work, we employ the weighted sum rule to combine the comparison scores obtained using R-ProCRC on the individual blocks I_{B_i} . Let $C_i = C_1, C_2, \dots, C_6$ denotes the comparison scores corresponding to i^{th} ear image block and $w_i = w_1, w_2, \dots, w_6$ denotes the weights then, the weighted sum rule can be written as:

$$F_c = \sum_{i=1}^6 w_i C_i; \text{ such that, } \sum_{i=1}^6 w_i = 1 \quad (20)$$

We propose to use the greedy algorithm to compute the optimized weights to achieve an improved ear verification performance. The proposed weight optimization begins with random initialization of the weights w_i such that $\sum_i w_i = 1$. Then, the fitness function is evaluated to check the desired optimization is achieved. The fitness function used in this work will compute $GMR@FAR =$

10^{-1} and the desired value of GMR is set to 100%. The weights are optimized in the subsequent iterations till it reached the maximum number of iteration (we have used 1000 iterations), or the desired value of GMR is achieved. Algorithm 2 illustrate the stepwise procedure of the proposed weighted scheme.

To generalize the weights computed using the proposed optimization scheme, we have used the independent database i.e. AMI Ear database ². We have used the ear samples corresponding to 50 subjects from the AMI Ear database to run the weight optimization scheme. Then, the optimized weights that are obtained using AMI Ear database are used in this work to evaluate the both surgery and non-surgery databases.

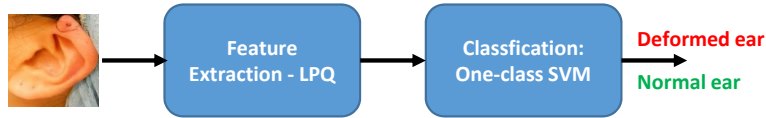


Figure 6: Block diagram of the proposed scheme for deformed ear detection

5. Proposed scheme for deformed and surgically altered ear detection

The idea of the proposed approach is to present a generalized approach to identify the subject with deformed and surgically modified ear to reduce the false reject. The standard approach to this problem is by defining and estimating the 2D ear image quality metrics or by using a traditional two class classifiers. Since it is very challenging to generalize the structural variation of the ear that makes the task of the 2D ear image definition and estimation harder. Furthermore, the limited availability of the deformed ear samples will always result in over-fitting problem in case of conventional 2-class classifiers. This motivates us to approach this issue using one-class classifiers to detect the deformed ear. Our approach can further be justified by the availability of the high number of normal (or non-deformed) 2D ear samples. Thus, the one-class classifier can be trained to produce a model for the normal ear (or positive data) that can decrease the overfitting problem.

Figure 6 shows the block diagram of the proposed scheme for deformed ear detection. The proposed approach can be structured in two functional blocks namely: feature extraction and one-class classification. In this work, we employed the rotation invariant Local Phase Quantization (LPQ) [37] as the feature

²<http://www.ctim.es/researchworks/ami ear database/>

extraction method by considering its insensitivity due to the imaging noise (blur or sharpness). LPQ features are obtained based on the local phase information extracted using the 2D Short-Time Fourier Transform (STFT) that are computed over the neighborhood region of the rectangular window. Figure 10 illustrates the qualitative results of the LPQ code image on both deformed (Figure 10 (a)) and normal ear (Figure 10 (b)) that indicate the visual differences in the LPQ coded features. In the next step, we employ the one-class Support Vector Machine (SVM) that uses the LPQ features to perform the classification [38]. The one-class SVM maximizes the separation between the points and the origin to perform the classification. Given the training data, the one-class SVM maps the data to high-dimension feature space then the kernel is used to compute the margin [38]. Finally, the one-class classification is performed to detect the outliers. In this work, we have used LIBSVM³ library for one-class SVM classifier and are trained using normal ear samples.

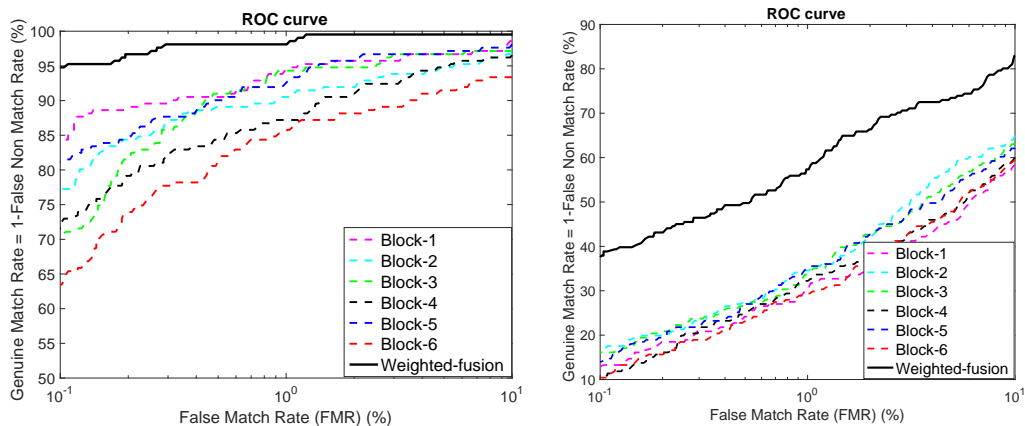
Table 1: Verification accuracy of SOTA and proposed algorithms on the non-surgery ear databases

Ear Verification Algorithms	Verification Rate (%)	
	GMR % @ FMR = 0.1%	EER(%)
Multi-resolution algorithm [39]	61.61	11.38
Local Phase Quantisation (LPQ) [37]	49.28	11.47
Binarised Statistical Image Features (BSIF) [40]	62.55	8.52
Log-Gabor features [41]	46.91	18.48
Local texture descriptor based on Radon transform [42]	57.81	5.21
Histogram of Oriented Gradients (HoG) [43]	65.87	7.58
Deep Learning: AlexNet	47.39	32.07
SURF [44]	24.28	14.76
Hybrid Fusion [25]	90.99	3.33
Proposed Method	94.78	0.95

6. Results and Discussion

This section presents and discusses the quantitative results of both proposed scheme for the ear verification and detection of the deformed ear on our newly developed ear surgery database.

³<https://www.csie.ntu.edu.tw/~cjlin/libsvm/>



(a) Verification performance of the proposed scheme on non-surgery ear database (IIT Delhi ear database) (b) Verification performance of the proposed scheme on surgery ear database (best viewed in color)

Figure 7: Verification performance of the proposed scheme. The dashed lines correspond to block processed results and thick line corresponds to final result.

6.1. Results on the proposed ear verification scheme

To study the effect of 2D ear surgery on the ear verification systems, we have selected nine different State-Of-The-Art (SOTA) ear verification algorithms for this study. These algorithms are: Multi-resolution algorithm using Local Binary Patterns (LBP) and Wavelet transform [39], Local Phase Quantisation (LPQ) [37], Binarised Statistical Image Features (BSIF) [40], Log-Gabor features [41], Local texture descriptor based on Radon transform [42], Histogram of Oriented Gradients (HoG) [43], key point descriptors such as SURF [44] and Hybrid fusion method particularly tailored for ear surgery verification using HoG and LPQ features proposed in [25]. These algorithms are chosen based on the proven accuracy and also based on their ability to cover a broad spectrum of local and global recognition techniques in the ear recognition literature.

In the spirit of recently reported performance of deep-learning techniques [45], we have explored a pre-trained deep CNN network - AlexNet to provide the comparison with proposed method. The pre-trained network is considered in this case owing to limited dataset availability in pre-and-post surgery conditions for each subject (one sample). As a specific note, in order to fully leverage the capability of deep networks, we perform data augmentation to generate 10 samples for each image in enrolment by inducing rotation and noise addition with various degrees. We then fine-tune the Alexnet on the augmented ear data by boosting the learning

rate of the last layer such that they change faster than the network. In this way, we do not modify the learning rates of the original layers as these are already significantly small. The learning rate used in the work are weight learning rate factor equaling to 10 and bias learning rate factor equaling to 20. To effectively evaluate the performance of the state-of-the-art techniques along with the proposed ear verification scheme we present two set of experiments such as (1) Performance on non-surgery ear database and (2) Performance on surgically altered ear database.

6.1.1. Performance on non-surgery ear database

This experiment is presented to analyze the performance of the baseline ear recognition algorithms along with the proposed scheme on the non-surgery ear database that is exhibiting similar characteristics to that of ear surgery database in terms of illumination, pose and number of subjects. Therefore, this experiment is performed on the publicly available non-surgery ear database - IIT Delhi Ear database [46]. In this database, we select first 211 data subjects such that each data subject will have 2 samples. Since each data subject is having two samples, we perform the experiments by considering one ear image as enrolment and another ear image as probe.

Figure 7a shows the verification performance of the proposed method interpreted with respect to individual blocks and the proposed weighted fusion. The proposed feature extraction and comparison scheme have indicated the outstanding performance with a verification rate of 94.78% @ FMR = 0.1%. It is also interesting to note that, the use of individual blocks such as block-1 has demonstrated the reasonable verification accuracy of 84.47% @ FMR = 0.1%. Further, the use of optimized weighted sum rule to combine the comparison scores from all six different blocks also indicated the improved verification performance. It

Table 2: Verification accuracy of SOTA and proposed algorithms on the surgery ear databases

Ear Verification Algorithms	Verification Rate (%)	
	GMR % @ FMR = 0.1%	EER(%)
Multi-resolution algorithm [39]	15.63	22.81
Local Phase Quantisation (LPQ) [37]	4.26	27.94
Binarised Statistical Image Features (BSIF) [40]	12.32	26.07
Log-Gabor features [41]	10.42	31.74
Local texture descriptor based on Radon transform [42]	12.79	28.01
Histogram of Oriented Gradients (HoG) [43]	22.27	22.74
Deep Learning: AlexNet	14.21	41.66
SURF [44]	1.42	32.33
Hybrid Fusion [25]	16.58	18.95
Proposed Method	37.44	14.22

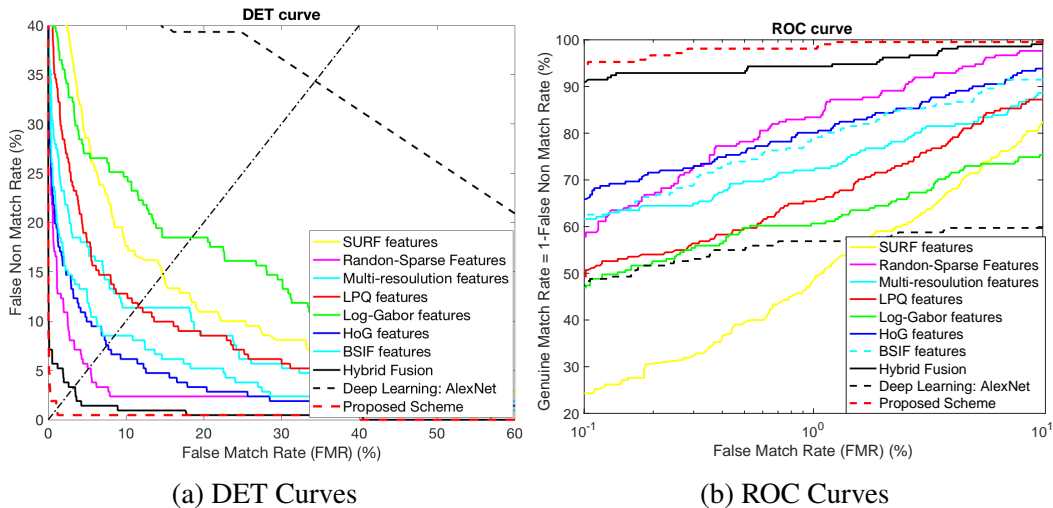


Figure 8: Comparative performance of the proposed scheme with SOTA on non-surgery ear database (IIT Delhi ear database)

can be further noted that the weight optimization is carried out on the independent database (see Section 4.4) and only the obtained optimized weights are used to get the final results of the proposed scheme. These obtained results justify the applicability of the proposed scheme for the single sample ear verification problem.

Figure 8 shows the comparative verification performance of the proposed scheme along with eight different State-Of-The-Art (SOTA) on the non-surgery ear database. The eight different SOTA algorithms are re-implemented (due to the lack of open source) and evaluated using our protocol that has one image for enrolment and one image for the probe. Table 1 indicates the quantitative results of the proposed and SOTA algorithms employed in this work. Based on the achieved results, the proposed scheme has emerged as the best method with the improved performance of $GMR = 94.78\% @ FMR = 0.1 \%$. These results indicate the efficacy of the proposed scheme, especially with the single enrolment sample.

6.1.2. Performance on ear surgery database

In this section, we present the quantitative results of the proposed and SOTA methods on the surgery ear database. In the lines of previous section, the protocol of evaluation remains with one sample (or image) for enrolment and one sample for the probe. Mainly, we enrolled the individuals with pre-surgery-image and obtained the performance by probing with the post-surgery-image.

Figure 7b shows the verification performance of the proposed method inter-

preted with respect to individual blocks and the weighted score fusion. The proposed feature extraction and comparison scheme have indicated the verification rate of 37.44% @ FMR = 0.1%. When compared to the performance of the individual blocks the optimized weighted sum rule has indicated the improved verification performance.

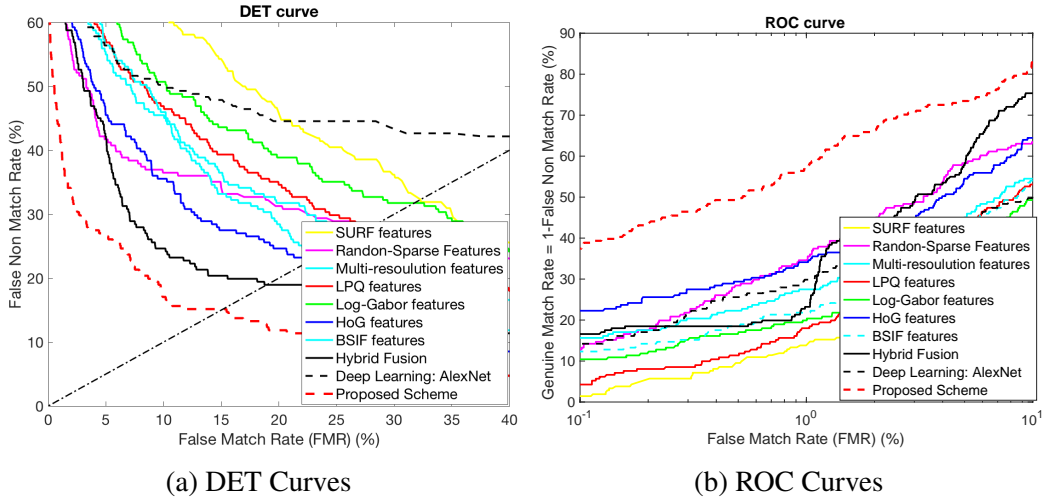


Figure 9: Comparative performance of the proposed scheme with SOTA on surgery ear database (best viewed in color)

Figure 9 shows the comparative verification performance of the proposed scheme along with eight different State-Of-The-Art (SOTA) on the surgery ear database. Table 2 indicates the quantitative results of the proposed and SOTA algorithms employed in this work. Based on the obtained results, the proposed scheme has shown the best performance with GMR = 37.44% at FMR = 0.1%. The improved performance of the proposed scheme can be attributed to the following facts:

- The proposed system can obtain invariant features from the bank of filters that primarily extract the localized edge descriptors learned using natural images.
- Further, the use of R-ProCRC boosts the classification performance by learning the probabilistic collaboration space from the feature space maximizing the inter-class distance.
- The use of non-overlapping block based approach and combining them at the comparison score level using optimised weights based on greedy al-

gorithm further contributes to the improved performance of the proposed scheme.

The degraded performance of the state-of-the-art methods can be mainly attributed to the nature of extracted features that are sub-optimal to the problem at the hand. It is noted from the results that, the use of both micro-texture and shape features fails drastically due to the deformation of the ear after surgery which do not correspond to images before surgery to a greater extent. As the shape based ear recognition techniques are mainly designed to match full shape of the ear, the verification performance decreases due to complete deformation of the shape after the surgery as anticipated.

Table 3: Verification accuracy of SOTA and proposed algorithms on lobe, beautification and helix surgery databases.

Ear Verification Algorithms	Ear Lobe Surgery		Beautification Surgery		Helix Surgery	
	GMR % @	EER(%)	GMR % @	EER(%)	GMR % @	EER(%)
	FMR = 0.1%		FMR = 0.1%		FMR = 0.1%	
Multi-resolution algorithm [39]	16.63	20.81	4.26	27.94	15.63	22.81
Local Phase Quantisation (LPQ) [37]	4.00	27.00	4.26	27.94	4.26	27.94
Binarised Statistical Image Features (BSIF) [40]	8.00	22.00	12.32	26.06	8.04	22.03
Log-Gabor features [41]	12.42	33.74	10.47	31.74	10.42	31.74
Local texture descriptor based on Radon transform [42]	10.00	24.02	9.16	27.24	7.69	28.20
Histogram of Oriented Gradients (HoG) [43]	16.00	25.57	16.00	25.57	16.00	25.57
Deep Learning: AlexNet	18.01	20.85	27.5	16.55	7.69	20.61
SURF [44]	1.96	29.31	1.67	33.36	2.56	31.41
Hybrid Fusion [25]	26.00	21.59	26.00	21.59	17.94	23.39
Proposed Method	39.05	18.97	37.67	14.16	35.89	20.59

The quantitative results obtained by both surgery and non-surgery ear database, it can be observed that (1) The performance of the SOTA scheme along with the proposed method has indicated the degraded results. This suggests the challenges of the recognizing the ear that are altered surgically. (2) The proposed method has demonstrated the improved performance on both surgically altered and non-surgical ear database.

6.1.3. Performance on individual ear surgery database

In this section, we present the evaluation results of the proposed and SOTA ear verification algorithms independently on three kinds of surgery such as Ear lobe, Beautification and Ear Helix.

Results on earlobe surgery. Table 3 shows the quantitative results of the ear recognition algorithms on ear lobe surgery database of 52 subjects. In this database, it is important to note that only ear lobe part has undergone the surgery, and helix

part of the ear will remain same with pre and post-surgery. The obtained results demonstrate the improved performance of the proposed scheme with GMR = 39.05% at FMR = 0.1%. The performance of the SOTA schemes has indicated a degraded performance when compared with the performance of the proposed method.

Results on ear beautification surgery. Table 3 shows the quantitative results of the ear recognition algorithms on ear beautification database comprised of 120 subjects. It can be noted here also that, the overall performance of the state-of-the-art ear recognition algorithms has demonstrated the degraded performance. The best performance is noted with the proposed scheme with GMR = 37.67% at FMR = 0.1%. In fact, this is the most natural case in real-life because, the data subject can enroll with the ear characteristics that is not completely deformed but may have small structural defects that can be treated with the Otoplasty to make ear beautiful. Hence, even though the ear biometric systems have very strict quality control in enrolling the ear samples, it will be challenging to discard these ear samples.

Results on ear Helix surgery. Table 3 shows the quantitative results of the ear recognition algorithms on ear helix database of 39 subjects. Most of the helix surgery samples included in our database corresponds to the surgery carried out on both mid and top helix portion of the ear. It can be noted here that, the overall performance of the state-of-the-art ear recognition algorithms has demonstrated the degraded performance. The best performance is noted with the proposed scheme with GMR = 35.89% at FMR = 0.1%.

Based on the obtained results as indicated in Table 3, the SOTA ear verification algorithms fail drastically to handle all three types of ear surgery. Among three different surgery databases, the helix surgery database has indicated a greater degradation. However, the performance of the proposed method has consistently shown an improved performance. Thus based on the extensive experiments carried out on both surgery and non-surgery ear database, the proposed scheme has emerged as the best scheme when compared with eight different state-of-the-art algorithms. This further justifies the applicability of the proposed scheme for the real-life ear verification applications.

6.2. Results on the proposed scheme with feature reduction

As the proposed scheme obtains high dimensional features obtained by convolving the ear patch image with the T-LCA filters, it is interesting to analyse the role of feature reduction techniques on the overall performance of the verification. To this extent, we have considered the Principal Component Analysis

(PCA) to reduce the dimension of feature space and then perform the verification. Table 4 indicates the performance of the proposed scheme with the feature space reduction using PCA for various dimensions of the features. The following are the main observations: (1) The performance of the proposed method with feature reduction techniques is comparable to the performance without feature reduction technique on the clean ear database (IIT-D ear database). With feature reduction, the proposed scheme indicates a performance with EER = 1.31% while without feature reduction scheme, the EER equals 0.95%. (2) The performance of the proposed scheme with feature reduction technique on the surgery ear database shows degraded performance when compared with the proposed method without feature reduction technique. Thus, the use of the feature reduction technique results in the loss of supplementary information that further degrades the overall performance of the proposed scheme. Thus, based on this analysis it can be observed that the use of feature reduction techniques can significantly reduce the feature space at the cost of degraded performance.

Table 4: Performance of the proposed scheme with feature dimensionality reduction using PCA

Table 5: IITD ear database

PC-Variance (%)	EER(%)	GMR(%) @FMR=0.1%	Feature Dimension
99 %	1.31	92.52	149
98 %	1.41	91.65	114
95 %	2.36	85.74	54
90 %	8.57	37.47	22

Table 6: Ear Surgery database

PC-Variance (%)	EER(%)	GMR(%) @FMR=0.1%	Feature Dimension
99 %	15.56	32.53	128
98 %	16.56	24.62	95
95 %	17.06	20.56	48
90 %	21.91	9.97	23

6.3. Computational complexity and execution time of the proposed technique

The proposed features extraction scheme is based on performing the 2D convolution of the ear images in a block-based manner with each of 256 T-LCF filters to derive the final feature vector. The off-line learning of T-LCF filters takes around 15 minutes based on the extracted features. Given the block image I_{Bi} of size $m \times n$ and the T-LCF filter size of $x \times y$, then the 2D convolution of I_{Bi} with a FB_k will result in $O(m \times n \times x \times y)$ operations. In our work, the ear image is of the dimension 30×30 with a T-LCF filter of dimension 16×16 . This will result in $30 \times 30 \times 16 \times 16 = 230400$ operations for one block corresponding to one filter. Thus, for the given ear image I , the proposed feature extraction technique will perform 353894400 operations. We have also computed the execution time of the proposed technique on the computer with i7 processor and 16GB RAM running on Matlab 2016b. The end-to-end execution of the proposed technique for

the given the test ear image of the ear I_{test} will take 6.89×10^{-3} seconds to render the verification score. However, an optimized code on other platforms (for e.g., C++) can improve the speed of execution.

6.4. Results on the proposed deformed and surgery ear detection scheme

This section presents the quantitative results of the proposed deformed ear detection scheme. Since the proposed system is based on the one-class classifier, we train the SVM classifier using clean (or normal) ear biometric database. In this work, we employ the normal ear images from publicly available ear databases such as IIT Delhi [46] and AMI ear database ⁴ to construct the training dataset. Thus, our training dataset is comprised of 500 ear images such that 456 ear images are taken from the IIT Delhi ear database and remaining ear images are taken from the AMI ear database. To choose the appropriate kernel and to tune its associated parameters, we have used a small ear database comprising of 80 ear images (44 from IIT Delhi ear database and remaining from AMI ear database) as the development database. We perform testing on three different experiments such as:

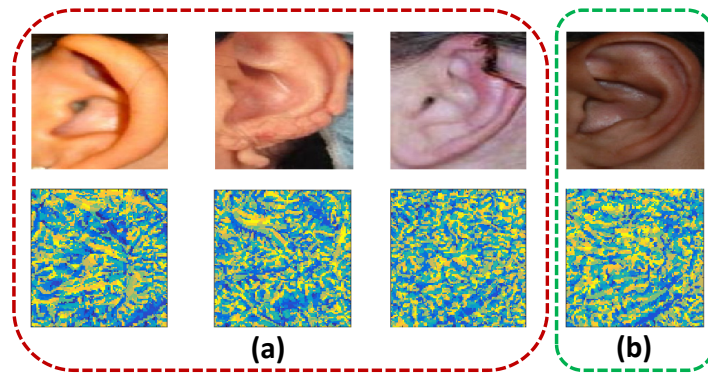


Figure 10: Qualitative results of the LPQ codes on (a) deformed ear (b) normal ear

Experiment 1: In this experiment, we consider testing ear images that corresponds to pre-surgery images. Since the ear images before surgery are normally deformed due to the various reasons such as wearing heavy ear-rings, accidents, the improper growth of the ear, etc, this experiment will provide the accuracy of the proposed method in detecting the deformed ear image. Thus, this analysis will

⁴<http://www.ctim.es/researchworks/amiocardatabase/>

use 211 ear images captured before surgery as the testing dataset.

Experiment 2: This experiment will evaluate the performance of the proposed scheme in correctly identifying the normal ear samples. Since biometric ear samples exhibit both inter and intra-variability, it is essential to understand the false rejection of the proposed scheme. To this extent, we have used 340 normal ear images (293 from IIT Delhi and 47 from AMI ear database) as the testing dataset.

Experiment 3: This experiment will evaluate the performance of the proposed scheme to detect surgically altered ears. Since the ear surgery process will alter both geometric and texture features of the ear, it can impact the overall appearance of the surgically altered ear when compared to the normal ear. To this extent, we use 211 ear images from post-surgery dataset to evaluate the performance of the proposed scheme and detect the surgically modified ears correctly.

Table 7 shows the quantitative results of the proposed scheme on three experiments described above. Since the proposed system employs the one-class SVM classifier, we have evaluated four different kernels whose parameters are tuned using development dataset. The performance of the proposed method is presented with test success rate, thus higher the value the better is the performance. As can be seen, the proposed scheme with polynomial kernel has consistently demonstrated the better performance in all three experiments. Even though the use of RBF and Sigmoid Kernels have shown better results than the polynomial kernel on Experiment-1 and Experiment-3, but show they have indicated a decreased performance in Experiment 2. The lower value of success rate in Experiment-2 indicates the increase in false reject of the normal ears. Thus, based on the obtained results, we can observe that the proposed scheme with polynomial kernel demonstrates the best performance on all three experiments with a success rate of 86.72% in detecting deformed ear, 72.25% in detecting normal ear and 84.83% in detecting the surgically modified ear.

Table 7: Performance of the proposed deformed ear detection scheme with four different kernels

Kernel	Test Success Rate (%)		
	Deformed Ear (Experiment 1)	Normal Ear (Experiment 2)	Surgery Ear (Experiment 3)
Linear	86.25	56.87	85.78
Polynomial	86.72	72.25	84.83
RBF	96.20	53.97	90.04
Sigmoid	94.78	48.17	95.73

7. Conclusion

Surgically modified ear recognition has been an unexplored area in the field of ear biometrics that poses various challenges. The increase in appearance consciousness in our population has increased the number of surgical procedures with the intention to beautify the lobe or helix or both, bring them to the original form or to restore symmetry. With the advancement in the technology and the affordability, people are undergoing ear surgery not only for the medical reason but also to improve the appearance to look beautiful. Since undergoing an ear lobe surgery will change both local as well as global appearance of the ear characteristic, this poses a new challenge in the 2D ear recognition. This paper introduces a comprehensive work in the field of ear surgery verification with the following contributions:

1. A new database is constructed with three different kinds of surgery which include ear lobe, ear helix and ear beatification. The created database is of 211 subjects with pre and post-surgery ear images.
2. Extensive experiments are presented to evaluate the performance of eight different state-of-the-art ear recognition algorithms quantitatively. Obtained comparative results indicate the algorithms' inability to mitigate the variation in the surgery which demonstrate the decreased performance when compared with non-surgery (or clean) ear database.
3. Proposed a novel scheme for ear verification based on the naturally inspired features learned using T-LCA and R-ProCRC. The proposed system has demonstrated the outstanding performance on both surgery and non-surgery ear database. This justifies its applicability to the real world applications.
4. Proposed a new scheme to detect the deformed ear based on LPQ and one-class SVM classifier. The proposed scheme not only detects the deformed ear with the success rate of 86.72% but also detects the surgically altered ear with a success rate of 84.83% and normal (or clean) ear with a success rate of 72.25%.

Based on the obtained results, we believe that more research is required to design optimal ear recognition algorithms that can account for the challenges due to surgery. The possible future work may include the use of new kind sensing devices such as Light Field camera or the Kinect to study the variation of depth information from normal to surgically modified ear image to identify the ear surgery sample more accurately and to improve the overall performance of the ear recognition system.

Appendix A

Table 8 shows the quantitative performance of the proposed scheme for rotation and translation on IIT-Delhi ear database. To evaluate the performance of the proposed scheme in this case, we keep the enrolled samples unaltered and probe samples are rotated to various degrees and translated (both vertically and horizontally). Based on the obtained results as indicated in the Table 8 following can be observed: (1) The proposed method has indicated good performance with the small variation in the rotation (up to 4°). However as the rotation angle increases, the performance of the proposed method decreases. (2) The proposed method has indicated good results with smaller translation (up to 2 X 2 pixels) in both horizontal and vertical direction. However, as the translation is increased, the performance also drops and the proposed approach did not show much variation in the performance between vertical and horizontal translation.

Table 8: Performance of the proposed scheme on image rotation and translation on IIT Delhi ear database

Rotation Angle (Degrees)	EER (%)
2	0.94
4	01.02
5	01.83
10	03.27

Verification performance versus image rotation

Translation type	Translation Pixels	EER (%)
Horizontal	2 X 2	0.98
	5 X 5	02.31
	10 X 10	03.62
Vertical	2 X 2	0.99
	5 X 5	01.89
	10 X 10	03.21

Verification performance versus image translation

Acknowledgment

This work is carried out under the funding of the Research Council of Norway (Grant No. IKTPLUS 248030/O70).

References

- [1] A. V. Iannarelli, Ear identification, Paramount Publishing Company, 1989.
- [2] A. Bertillon, La photographie judiciaire: avec un appendice sur la classification et l'identification anthropométriques, Gauthier-Villars, 1890.

- [3] P. Yan, K. Bowyer, Empirical evaluation of advanced ear biometrics, in: IEEE CVPR-Workshops 2005, 2005, pp. 41–41.
- [4] M. Burge, W. Burger, Ear biometrics, in: Biometrics, Springer, 1996, pp. 273–285.
- [5] S. Ansari, P. Gupta, Localization of ear using outer helix curve of the ear, in: ICCTA'07, IEEE, 2007, pp. 688–692.
- [6] E. Said, A. Abaza, H. Ammar, Ear segmentation in color facial images using mathematical morphology, in: Biometrics Symposium, 2008. BSYM'08, 2008, pp. 29–34.
- [7] T. Yuizono, Y. Wang, K. Satoh, S. Nakayama, Study on individual recognition for ear images by using genetic local search, in: wcci, 2002, pp. 237–242.
- [8] B. Arbab-Zavar, M. S. Nixon, On shape-mediated enrolment in ear biometrics, in: Advances in visual computing, 2007, pp. 549–558.
- [9] S. Prakash, U. Jayaraman, P. Gupta, A skin-color and template based technique for automatic ear detection, in: 7th ICAPR'09, 2009, pp. 213–216.
- [10] D. Watabe, H. Sai, K. Sakai, O. Nakamura, Ear biometrics using jet space similarity, in: Electrical and Computer Engineering, 2008. CCECE 2008. Canadian Conference on, 2008, pp. 001259–001264.
- [11] A. H. Cummings, M. S. Nixon, J. N. Carter, A novel ray analogy for enrolment of ear biometrics, in: 4th IEEE - BTAS, 2010, 2010, pp. 1–6.
- [12] H. Chen, B. Bhanu, Human ear recognition in 3d, IEEE Transactions on PAMI 29 (4) (2007) 718–737.
- [13] S. M. Islam, M. Bennamoun, R. Davies, Fast and fully automatic ear detection using cascaded adaboost, in: IEEE WACV 2008., 2008, pp. 1–6.
- [14] A. Abaza, C. Hebert, M. A. F. Harrison, Fast learning ear detection for real-time surveillance, in: 4th IEEE BTAS - 2010, 2010, pp. 1–6.
- [15] L. Chen, Z. Mu, Partial data ear recognition from one sample per person, IEEE Transactions on Human-Machine Systems 46 (6) (2016) 799–809.

- [16] M. Kumar, A. Insan, N. Stoll, K. Thurow, R. Stoll, Stochastic fuzzy modeling for ear imaging based child identification, *IEEE Transactions on Systems, Man, and Cybernetics: Systems* 46 (9) (2016) 1265–1278.
- [17] S. Tiwari, S. Kumar, S. Kumar, G. R. Sinha, Ear recognition for newborns, in: *2015 2nd International Conference on Computing for Sustainable Global Development (INDIACom)*, 2015, pp. 1989–1994.
- [18] A. Pflug, C. Busch, Ear biometrics: a survey of detection, feature extraction and recognition methods, *Biometrics, IET* 1 (2) (2012) 114–129.
- [19] Z. Emersic, V. Struc, P. Peer, Ear recognition: More than a survey, *Neurocomputing* 255 (2017) 26 – 39, *bioinspired Intelligence for machine learning*.
- [20] A. Abaza, A. Ross, C. Hebert, M. A. F. Harrison, M. S. Nixon, A survey on ear biometrics, *ACM computing surveys (CSUR)* 45 (2) (2013) 22.
- [21] S. M. Islam, M. Bennamoun, R. Owens, R. Davies, Biometric approaches of 2d-3d ear and face: A survey, in: *Advances in computer and information sciences and engineering*, 2008, pp. 509–514.
- [22] M. Choraś, Image feature extraction methods for ear biometrics—a survey, in: *CISIM’07*, 2007, pp. 261–265.
- [23] K. Pun, Y. Moon, Recent advances in ear biometrics, in: *IEEE Int. Conf. on Automatic Face and Gesture Recognition*, 2004, pp. 1–4.
- [24] K. Ramesh, K. N. Rao, Pattern extraction methods for ear biometrics-a survey, in: *2009 World Congress on Nature&Biologically Inspired Computing (NaBIC)*, 2009.
- [25] R. Raghavendra, K. B. Raja, C. Busch, Ear recognition after ear lobe surgery: A preliminary study, in: *IEEE ISBA 2016*, 2016, pp. 1–6, (To be published in March 2016).
- [26] K. Kavukcuoglu, R. Fergus, Y. LeCun, et al., Learning invariant features through topographic filter maps, in: *Computer Vision and Pattern Recognition*, 2009. *CVPR 2009. IEEE Conference on*, 2009, pp. 1605–1612.
- [27] Y. Jia, S. Karayev, Self-organizing sparse codes.

- [28] C. Rozell, D. Johnson, R. Baraniuk, B. Olshausen, Locally competitive algorithms for sparse approximation, in: 2007 IEEE International Conference on Image Processing, Vol. 4, 2007, pp. IV–169.
- [29] S. Cai, L. Zhang, W. Zuo, X. Feng, A probabilistic collaborative representation based approach for pattern classification, in: IEEE Conference on Computer Vision and Pattern Recognition, (CVPR 2016), 2016.
- [30] J. Niamtu, Eleven pearls for cosmetic earlobe repair, *Dermatologic surgery* 28 (2) (2002) 180–185.
- [31] R. Singh, M. Vatsa, H. Bhatt, S. Bharadwaj, A. Noore, S. Nooreydzan, Plastic surgery: A new dimension to face recognition, *IEEE Transactions on IFS* 5 (3) (2010) 441–448.
- [32] G. B. Huang, M. Ramesh, T. Berg, E. Learned-Miller, Labeled faces in the wild: A database for studying face recognition in unconstrained environments, Tech. Rep. 07-49, University of Massachusetts, Amherst (2007).
- [33] J. Ngiam, Z. Chen, S. A. Bhaskar, P. W. Koh, A. Y. Ng, Sparse filtering, in: *Advances in NIPS*, 2011, pp. 1125–1133.
- [34] W. E. Hahn, S. Lewkowicz, D. C. Lacombe Jr, E. Barenholtz, Deep learning human actions from video via sparse filtering and locally competitive algorithms, *Multimedia Tools and Applications* 74 (22) (2015) 10097–10110.
- [35] D. C. LaCombe Jr, Topographic locally competitive algorithm.
- [36] A. Hyvärinen, J. Hurri, P. O. Hoyer, *Natural Image Statistics: A Probabilistic Approach to Early Computational Vision.*, Vol. 39, Springer Science & Business Media, 2009.
- [37] V. Ojansivu, E. Rahtu, J. Heikkila, Rotation invariant local phase quantization for blur insensitive texture analysis, in: 19th International Conference on Pattern Recognition, 2008, pp. 1–4.
- [38] H. J. Shin, D.-H. Eom, S.-S. Kim, One-class support vector machines an application in machine fault detection and classification, *Computers & Industrial Engineering* 48 (2) (2005) 395 – 408.

- [39] Y. Wang, Z.-c. Mu, H. Zeng, Block-based and multi-resolution methods for ear recognition using wavelet transform and uniform local binary patterns, in: ICPR 2008, 2008, pp. 1–4.
- [40] A. Benzaoui, A. Hadid, A. Boukrouche, Ear biometric recognition using local texture descriptors, *Journal of Electronic Imaging* 23 (5) (2014) 053008–053008.
- [41] B. Arbab-Zavar, M. S. Nixon, Robust log-gabor filter for ear biometrics, in: ICPR 2008, 2008, pp. 1–4.
- [42] A. Kumar, T.-S. T. Chan, Robust ear identification using sparse representation of local texture descriptors, *Pattern recognition* 46 (1) (2013) 73–85.
- [43] N. Damer, B. Fuhrer, Ear recognition using multi-scale histogram of oriented gradients, in: 2012 8th IHH-MSP, 2012, pp. 21–24.
- [44] S. Prakash, P. Gupta, An efficient ear recognition technique invariant to illumination and pose, *Telecommunication Systems* 52 (3) (2013) 1435–1448.
- [45] P. L. Galdmez, W. Raveane, A. G. Arrieta, A brief review of the ear recognition process using deep neural networks, *Journal of Applied Logic* 12 (2) (2016) 1–12.
- [46] Automated human identification using ear imaging, *Pattern Recognition* 45 (3) (2012) 956 – 968.